Journal of Luminescence 129 (2009) 1619–1624

Contents lists available at ScienceDirect

Journal of Luminescence

journal homepage: www.elsevier.com/locate/jlumin

Effects of annealing on the structure and photoluminescence of ZnO-sputtered coaxial nanowires

Hyoun Woo Kim *, Mesfin Abayneh Kebede, Hyo Sung Kim, Myung Ho Kong, Chongmu Lee

Division of Materials Science and Engineering, Inha University, Incheon 402-751, Republic of Korea

ARTICLE INFO

Available online 5 April 2009

Keywords:
ZnO
Nanowires
Thermal annealing

ABSTRACT

We reported the preparation and annealing effects of Zinc oxide ZnO/SiO_x core–shell nanowires, in which ZnO shell layers were deposited by sputtering. Based on scanning electron microscopy, transmission electron microscopy, X-ray diffraction, and photoluminescence (PL) investigations, we monitored structural and optical changes with respect to the post-annealing process. The samples were mostly amorphous with some crystalline ZnO structure, whereas annealing at 900–1000 °C reduced the amount of Zn elements. Thermal annealing induced change in the shape of the PL emission spectra.

1. Introduction

Heterostructures contribute significantly to fundamental research and practical devices, with which nanoscaled electronic devices with a variety of functions can be realized [1]. Up to now,, several researchers have reported on the two-dimensional (2D) heterostructures consisting of mutilayer thin films, as well as zero-dimensional (0D) heterostructures including quantum dots or nanocrystals. In recent years, there have been great interests in the fabrication of coaxial nanocable-like one-dimensional (1D) structures, which combine the different types of nanotubes and nanowires in axial or radial directions [2,3].

Zinc oxide (ZnO) is of great interest because it has wide direct band gap (3.37 eV) and large exciton binding energy (60 meV), and thus has electronic and photonic applications [4]. Furthermore, with its versatile and useful properties, ZnO can be used in piezoelectric transducers and actuators, hydrogen storage, sensors, solar cells, and photo catalysts [5]. On the other hand, SiO_x has been intensively studied as an important photoluminescence (PL) material [6,7]. Furthermore, SiO_x core nanowires are known to be one of the most appropriate materials as sacrificial templates for the fabrication of tubular nanostructures, owing to their smooth surface, high thermal stability, and good removability [8].

In this paper, we have demonstrated the fabrication of SiO_x–ZnO core–shell nanowires, in which the ZnO shell layers were coated on SiO_x core nanowires by DC magnetron sputtering. In addition, we have carried out the thermal annealing, comparatively investigating the core–shell nanowires depending on the annealing temperature. Thermal annealing is not only an important step in the fabrication of integrated circuit (IC) devices, but also is able to modify or improve the properties of as-synthesized core–shell nanowires.

2. Experimental

To prepare core SiO_x nanowires in a tube-furnace, we have employed Ag (approximate thickness = 9 nm)-coated Si substrates, which were heated at 1050 °C for 2 h, in an air flow (~3.15% O_2 in a balance of argon (Ar)). Coating experiments on the core SiO_x nanowires were conducted using a DC magnetron sputter system, in a mixture of Ar and O_2 gases. The flow rates of Ar and O_2 gases were 30 and 10 sccm, respectively. With supplying 70 W RF power at 13.56 MHz, a ZnO (99.99% purity) target has been used. The ZnO shell layer was deposited for 6 min at room temperature. Subsequently, samples were annealed for 30 min at temperatures in the range of 500–1000 °C. As an ambient gas, Ar was flowed at 2 Torr.

The resulting samples were characterized by means of X-ray diffraction (XRD) (Philips X'pert MRD diffractometer with CuKα radiation), field emission scanning electron microscopy (FE-SEM) (Hitachi, S-4200), and transmission electron microscopy (TEM) (Philips, CM-200) with energy-dispersive X-ray spectroscopy (EDX) equipped. PL was conducted at room temperature with the 325 nm line from a He–Cd laser (Kimon, 1 K, Japan). The SPEC-1403 spectrometer was used.

3. Results and discussion

Fig. 1a–d show XRD spectra of as-fabricated SiO_x–ZnO core–shell nanowires, SiO_x–ZnO core–shell nanowires annealed

* Corresponding author. Tel.: +82 32 860 7544.
E-mail address: hwkim@inha.ac.kr (H.W. Kim).

0022-2313/$ - see front matter © 2009 Elsevier B.V. All rights reserved.
doi:10.1016/j.jlumin.2009.03.030

at 500, 800, and 1000 °C, respectively. Owing to the absence of a strong ZnO diffraction peak, it is supposed that the deposit is mainly the amorphous phase. However, a weak line is found to coincide with the (1 1 0) peak of the hexagonal structure of ZnO (JCPDS File no. 05-0664). In addition, in annealed samples, some peaks can be clearly indexed to the (1 0 1) and (1 0 2) reflection of the hexagonal structure of ZnO (JCPDS File no. 05-0664).

Fig. 2a and b show SEM and TEM images of as-fabricated SiO_x–ZnO core–shell nanowires, respectively, revealing the production of 1D nanomaterials. Fig. 2c is corresponding selected area electron diffraction (SAED) pattern. Although the nanostructure is overall amorphous from the highly dispersed SAED pattern, the existence of very weak diffraction rings suggest that there exists a small fraction of crystalline ZnO phase. Fig. 2d exhibits an enlarged TEM image from a marked area in Fig. 2b. It is shown that the nanowire has a mixture of amorphous and crystalline phases, which is consistent with the SAED pattern. In crystalline regions, the lattice spacing is measured to be 0.25 nm, corresponding to (1 0 1) planes of hexagonal ZnO. Fig. 2e exhibits line concentration profiles for Si, O, and Zn, respectively, along the line drawing across the diameter of a SiO_x–ZnO core–shell nanowire. While Si element is encountered in the core of the coaxial nanowires, it is worth noting that Zn is mainly located at the sheath region, which can be evidenced by a valley-like profile.

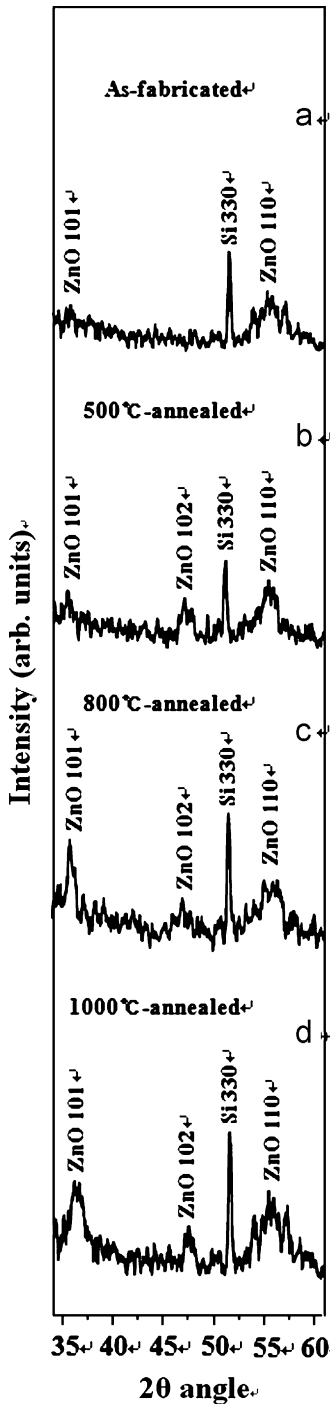

Fig. 1. XRD patterns of (a) as-fabricated SiO_x–ZnO core–shell nanowires and (b, c,and d) SiO_x–ZnO core–shell nanowires annealed at (b) 500 °C, (c) 800 °C, and (d) 1000 °C.

Fig. 3a shows SEM and TEM images of 500 °C-annealed SiO_x–ZnO core–shell nanowires, respectively, exhibiting a 1D morphology. Fig. 3c is an associated SAED pattern, indicating the existence of ZnO diffraction rings. In the SAED pattern, the ZnO structure was indexed according to the following procedure. For example, since $rd = L\lambda$, where r, d, and $L\lambda$ were ring pattern radius, interplanar distance, and camera constant, respectively, by inserting the camera constant of 19.34 Å mm and the ring pattern radius of 6.9 mm, we have obtained the d-value of about 2.8 Å. This value corresponds to d_{100} value of 2.8 Å of hexagonal ZnO structure (JCPDS File no. 05-0664). By comparing Fig. 3c with Fig. 2c, we observe that the overall area of the halo in the SAED pattern was reduced and the diffraction rings became clearer by the thermal annealing. It is possible that a little fraction of amorphous ZnO phase has been transformed to the crystalline phase. TEM–EDX measurement taken at the nanowire of Fig. 3b indicates that it comprises Zn elements (Fig. 3d), whereas the Cu signal comes from the Cu grid. A high-resolution TEM (HRTEM) image from a squared area in Fig. 3b is shown in Fig. 3e, indicating that the 500 °C-annealed sample is polycrystalline. The distance between two neighboring fringes is about 0.28 nm, coinciding with the interplanar distance of the (1 0 0) plane of the hexagonal ZnO phase. Since XRD investigation revealed the generation of Zn_2SiO_4 phase upon the thermal annealing, the Zn_2SiO_4 phase should be localized in the boundaries between SiO_x core and ZnO shell layers. Fig. 3f and g shows low-magnification and lattice-resolved TEM images of 900 °C-annealed SiO_x–ZnO core–shell nanowires, respectively, indicating that the nanowire is of amorphous structure. Fig. 3h shows line concentration profiles for Si, O, and Zn, respectively, along the line drawing across the diameter of a 900 °C-annealed SiO_x–ZnO core–shell nanowire. By comparing Fig. 3h with Fig. 2e, we observe that the Zn concentration has been noticeably reduced. Also, by comparing Fig. 3i with d, the amount of Zn elements has been significantly decreased by increasing the annealing temperature from 500 to 900 °C.

Fig. 4a shows the PL emission spectrum of the core SiO_x nanowires upon photoexcitation at 3.82 eV. By Gaussian deconvolution, the overall feature exhibits two emission bands centered at 2.4 eV in the green region and 2.9 eV in the blue region, respectively. Both blue and green light emissions can be attributed to oxygen deficiency-related defects [9–11]. Fig. 4b shows the PL spectrum of 500 °C-annealed SiO_x–ZnO core–shell nanowires. Apart from the SiO_x-associated 2.4 and 2.9 eV peaks, there exists an additional green emission peak (~2.3 eV) from ZnO, being related to deep trapping sites by defects such as oxygen vacancies [12–16]. By comparing Fig. 4b with a, we reveal that the PL intensities of 2.4 and 2.9 eV peaks were significantly reduced by the ZnO-coating and subsequent thermal annealing. We surmise that the reduction is related to the covering effect of ZnO shell layer. Fig. 4c and d show PL spectra of the SiO_x–ZnO

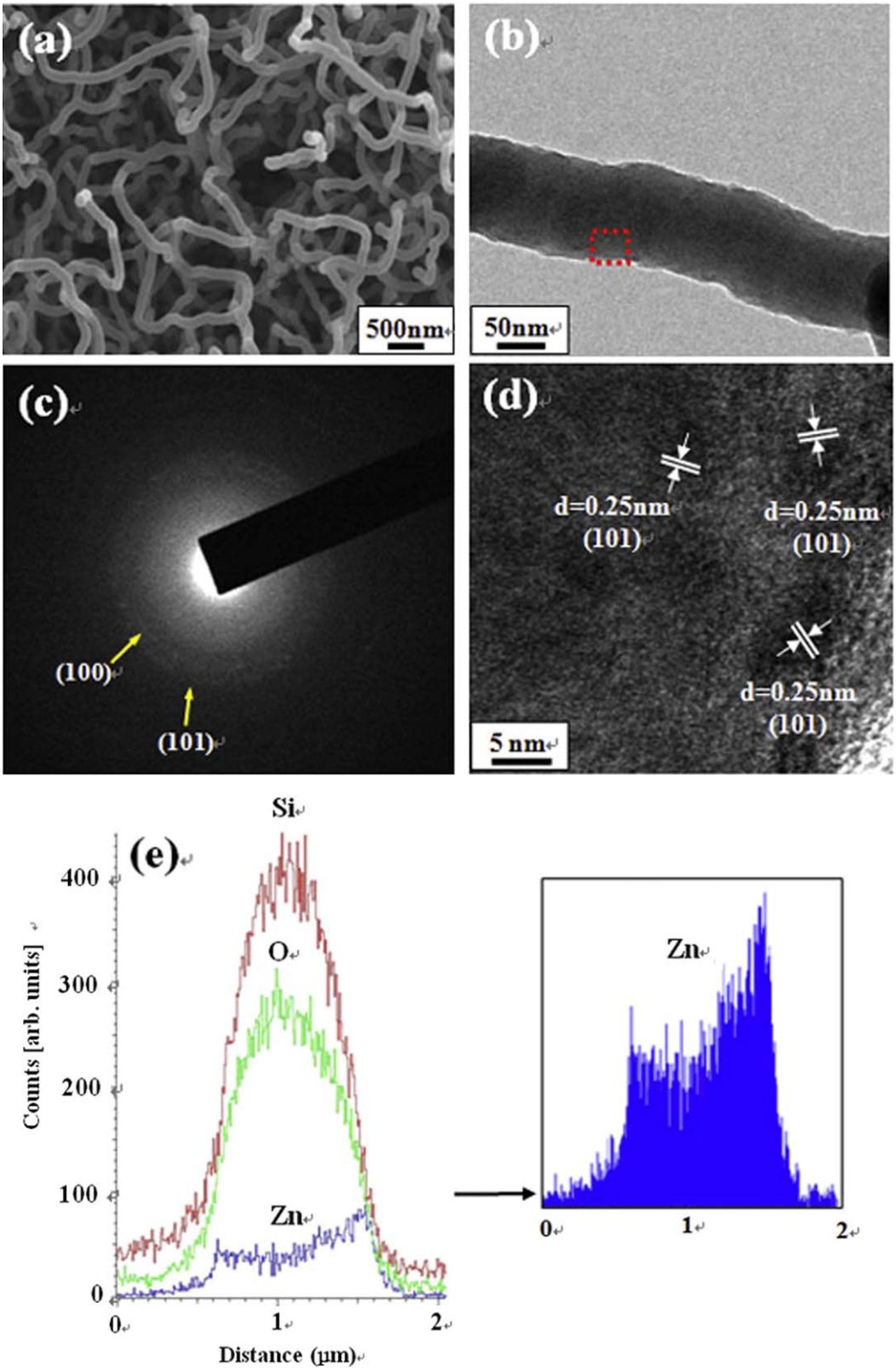

Fig. 2. (a) SEM and (b) TEM images of as-fabricated SiO_x–ZnO core–shell nanowires. (c) Corresponding selected area electron diffraction (SAED) pattern. (d) Enlarged TEM image from a marked area in (b). (e) TEM–EDX line concentration profiles for Si, O, and Zn, respectively, along the line drawing across the diameter of an as-fabricated SiO_x–ZnO core–shell nanowire.

core–shell nanowires annealed at 800 and 900 °C, respectively. It is observed that the intensities of both 2.4 and 2.9 eV bands tend to increase with increasing the annealing temperature in the range 500–900 °C. Since both 2.4 and 2.9 eV bands are related to oxygen deficiency, it is likely that high-temperature annealing enhanced the oxygen vacancies, intensifying the 2.4 and 2.9 eV

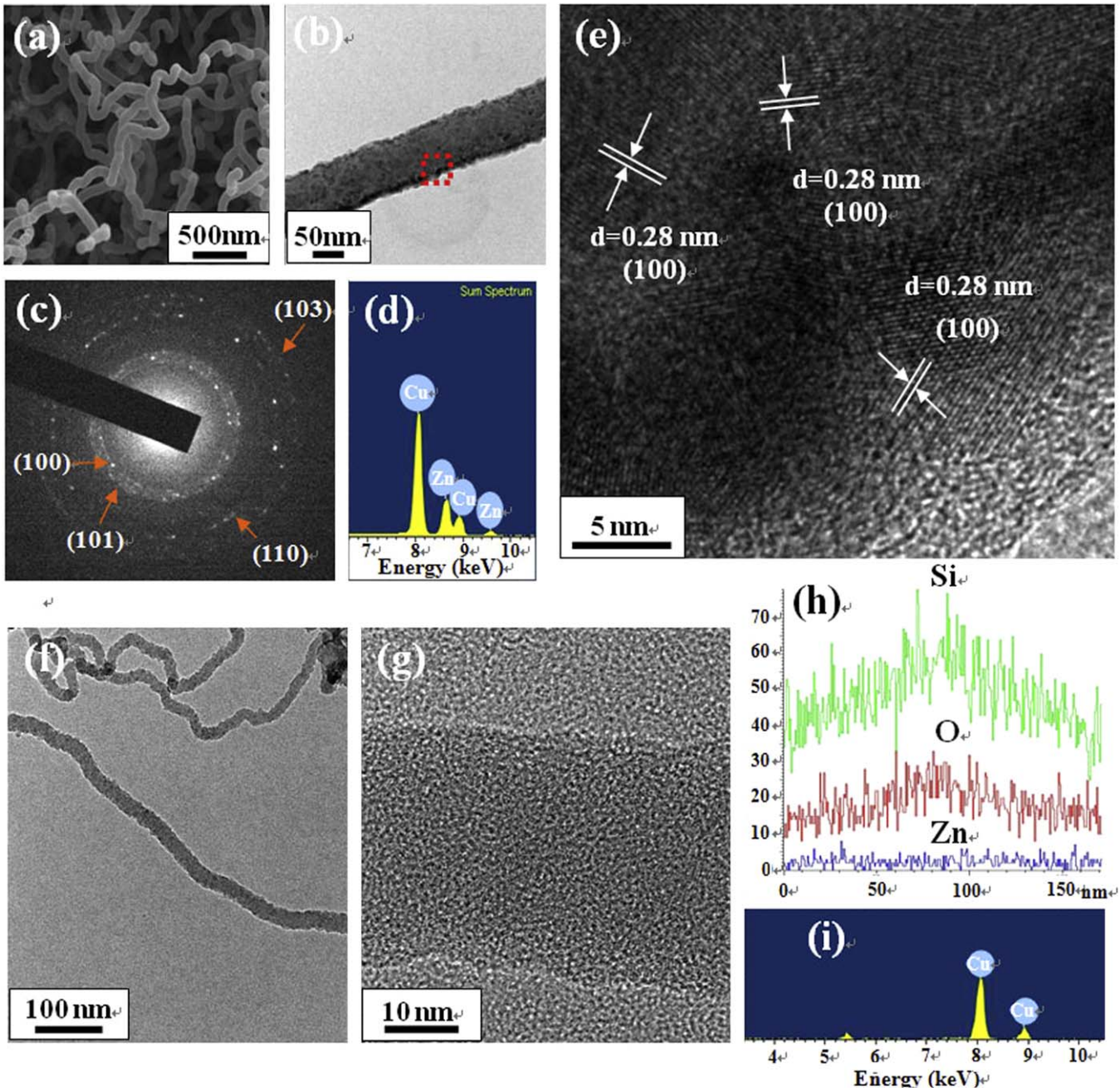

Fig. 3. (a) SEM and (b) TEM images of 500 °C-annealed SiO_x–ZnO core–shell nanowires. (c) Associated SAED pattern. (d) TEM–EDX measurement taken at the nanowire of (b). (e) HRTEM image enlarging the area enclosed by a square box in (b). (f) Low-magnification. (g) Lattice-resolved TEM images of 900 °C-annealed SiO_x–ZnO core–shell nanowires. (h) TEM–EDX line concentration profiles for Si, O, and Zn, respectively, along the line drawing across the diameter of a 900 °C-annealed SiO_x–ZnO core–shell nanowire. (i) TEM–EDX spectrum from 900 °C-annealed SiO_x–ZnO core–shell nanowires.

bands. In addition, it is noteworthy that the PL intensity of the 2.3 eV-centered peak is decreased with increasing the annealing temperature. This can be associated with observation that the amounts of Zn elements were reduced after the annealing at 900 °C (Fig. 3i). Although the associated mechanism has not yet been clarified, it is well known that the decomposition of ZnO occurs at sufficiently high temperatures [17]. Solid ZnO can be sublimated to ZnO vapor, part of which can decompose into Zn and O_2 vapors [17]. Further detailed study is in progress.

4. Conclusions

In conclusion, the effect of annealing temperature on the structure and luminescence of core SiO_x/shell ZnO nanowires has been studied for the first time. The 500 °C-annealed SiO_x–ZnO core–shell nanowires exhibited the existence of a hexagonal ZnO phase. PL emission spectra of the core SiO_x/shell ZnO nanowires comprise three emission bands, centered at 2.3, 2.4, and 2.9 eV. While 2.4 and 2.9 eV bands are ascribed to SiO_x core, 2.3 eV band is attributed to ZnO and/or Zn_2SiO_4 phase. We have discussed the

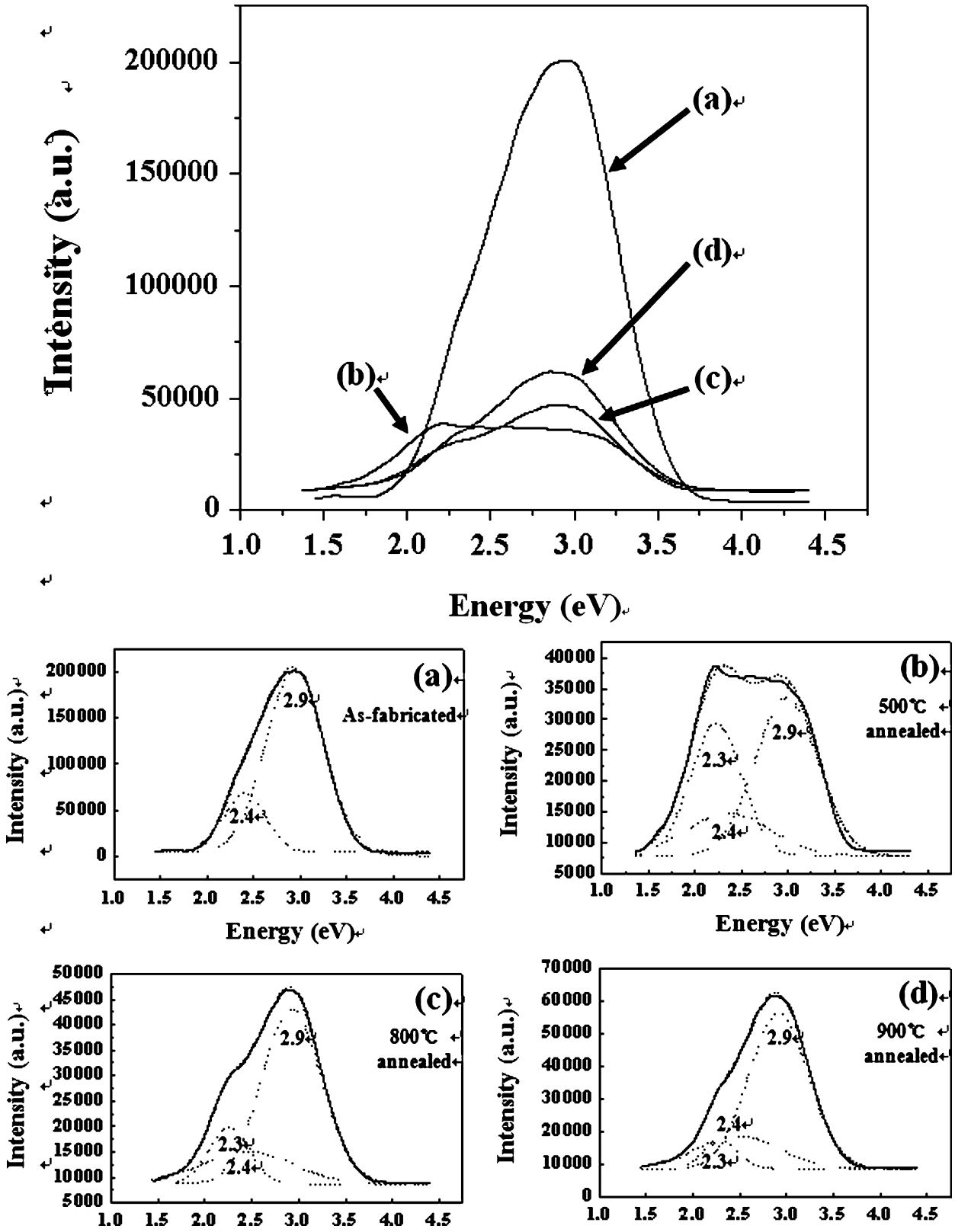

Fig. 4. PL spectrum of (a) as-fabricated SiO_x–ZnO core–shell nanowires and (b–d) annealed SiO_x–ZnO core–shell nanowires. The annealing temperature was set to (b) 500 °C, (c) 800 °C, and (d) 900 °C.

mechanism by which the relative intensity of 2.3 eV-centered band is decreased by increasing the annealing temperature. This study will give an insight into the annealing studies of various coaxial heteronanowires.

Acknowledgements

This work was supported by Korea Research Foundation Grant funded by the Korean Government (MOEHRD) (KRF-2007-521-

D00216). The main calculations were performed by the supercomputing resources of the Korea Institute of Science and Technology Information (KISTI).

References

[1] H.M. Lin, Y.-L. Chen, J. Yang, Y.-C. Liu, K.-M. Yin, J.-J. Kai, F.-R. Chen, L.-C. Chen, C.-C. Chen, Nano Lett. 3 (2003) 537.
[2] Y. Zhang, K. Suenaga, C. Colliex, S. Iijima, Science 281 (1998) 973.
[3] W.-S. Shi, H.-Y. Peng, L. Xu, N. Wang, Y.-H.H. Tang, S.-T. Lee, Adv. Mater. 12 (2000) 1927.
[4] W.D. Yu, X.M. Li, X.D. Gao, P.S. Qiu, W.X. Cheng, A.L. Ding, Appl. Phys. A 79 (2004) 453.
[5] A. Umar, B.-K. Kim, J.-J. Kim, Y.B. Hahn, Nanotechnology 18 (2007) 175606.
[6] H. Nishikawa, T. Shiroyama, R. Nakamura, Y. Ohiki, K. Nagasawa, Y. Hama, Phys. Rev. B 45 (1992) 586.
[7] L.S. Liao, X.M. Bao, X.Q. Zhang, N.S. Li, N.B. Min, Appl. Phys. Lett. 68 (1996) 850.
[8] S.L. Cheng, W.C. Hslao, Electrochem. Solid-State Lett. 10 (2007) D142.
[9] D.P. Yu, Q.L. Hang, Y. Ding, H.Z. Zhang, Z.G. Bai, J.J. Wang, Y.H. Zou, W. Qian, G.C. Xiong, S.Q. Feng, Appl. Phys. Lett. 73 (1998) 3076.
[10] H. Nishikawa, T. Shiroyama, R. Nakamura, Y. Ohiki, K. Nagasawa, Y. Hama, Phys. Rev. B 45 (1992) 586.
[11] J.Q. Hu, Y. Jiang, X.M. Meng, C.S. Lee, S.T. Lee, Chem. Phys. Lett. 367 (2003) 339.
[12] J.S. Kang, H.S. Kang, S.S. Pang, E.S. Shim, S.Y. Lee, Thin Solid Films 443 (2003) 5.
[13] P. Yang, H. Yan, S. Mao, R. Russo, J. Johnson, R. Saykally, N. Morris, J. Pham, R. He, H.-J. Choi, Adv. Funct. Mater. 12 (2002) 323.
[14] Q. Wan, Z.T. Song, W.L. Liu, C.L. Lin, T.H. Wang, Nanotechnology 15 (2004) 559.
[15] D.C. Reynolds, D.C. Look, B. Jogai, C.W. Litton, T.C. Collins, W. Harsch, G. Cantwell, Phys. Rev. B 57 (1998) 12151.
[16] S.W. Jung, W.I. Park, H.D. Cheong, G.-C. Yi, H.M. Jang, S. Hong S, T. Joo, Appl. Phys. Lett. 80 (2002) 1924.
[17] X.Y. Kong, Y. Ding, Z.L. Wang, J. Phys. Chem. B 108 (2004) 570.